

Research Article

Rapid Biosynthesis of Gold Nanoparticles by the Extracellular Secretion of *Bacillus niabensis* 45: Characterization and Antibiofilm Activity

Yumei Li, Yamei Li, Qiang Li, Xiangyu Fan, Juan Gao, and Yan Luo

School of Biological Science and Biotechnology, University of Jinan, Jinan, China

Correspondence should be addressed to Yumei Li; mls_liym@ujn.edu.cn

Received 19 May 2016; Accepted 21 July 2016

Academic Editor: Roberto Comparelli

Copyright © 2016 Yumei Li et al. This is an open access article distributed under the Creative Commons Attribution License, which permits unrestricted use, distribution, and reproduction in any medium, provided the original work is properly cited.

The present study demonstrated that the extracellular biosynthesis of gold nanoparticles (GNPs) using *B. niabensis* 45 may be mediated by a cyclic peptide (P2). The molecular weight of P2 was determined to be about 1122 Da by MALDI-TOF-MS and ESI-MS. A novel protocol for rapid biosynthesis of GNPs using P2 was developed. The results showed that GNP synthesis could be completed in a wide range of temperatures (40–100°C) and pH (6.0–10.0) within few minutes when 9 mL of P2 (2 mg/mL) and 1 mL of HAuCl₄ solution (2 mM) were mixed together. The synthesized GNPs were further characterized. Energy dispersive spectroscopy (EDS) and X-ray diffraction (XRD) analysis confirmed the presence of elemental gold and crystalline structure of the GNPs, respectively. Scanning electron microscopy (SEM) and transmission electron microscopy (TEM) revealed the formation of spherical metallic GNPs. The size distribution of GNPs calculated using ImageJ software was found to be 10–20 nm. And these GNPs showed excellent antibiofilm activity against *Pseudomonas aeruginosa* PAO1 and *Staphylococcus aureus* ATCC25923. The results revealed microbial cyclic peptides could be used as synthesis of GNPs which had potent antibiofilm potential.

1. Introduction

Gold nanoparticles (GNPs) have unique optical, electrical, and photothermal properties [1]. They have been extensively employed in biomedical field in the last decade like drug delivery, imaging, and treatment of major life threatening diseases [2, 3]. Nevertheless, experimental use of GNPs presented possible medical hazards which could threaten human health because of their surface properties [4]. So there is an urgent need to develop safe, clean, nontoxic, and environment-friendly method of GNP synthesis. Biological approaches are available for synthesis of GNPs. Biosynthesized GNPs are frequently attached to a biological carrier or scaffold and many feature biogenic capping materials that enhance the compatibility and stability of GNPs under environmental conditions. Several bacteria, actinomycetes, fungi, and plants exhibit the excellent ability to produce GNPs intracellularly and/or extracellularly [5]. The shape and size of the GNPs synthesized by the biological systems can

be affected by some parameters such as pH, temperature, substrate concentrations, and reaction time [6].

Although great many reports focus on microbial synthesis of GNPs, the mechanistic aspects have not been clarified and the active ingredients controlling GNP synthesis need to be studied in depth [7–9]. Such studies have been performed to isolate the active ingredient and explain the mechanism underlying GNP synthesis. The organic phosphate compounds from *B. subtilis* 168 may be as bacteria-Au complexing agents to lead to the formation of GNPs [7]. The species specific NADH dependent reductases from *Fusarium oxysporum* and *Rhodopseudomonas capsulata* could mediate bioreduction of Au³⁺ ions to carry out the synthesis of GNPs [8–10]. The lignolytic enzymes such as laccase and ligninase from *Phanerochaete chrysosporium* were reported to synthesize extracellular and intracellular GNP synthesis [11]. In addition, the proteins, polysaccharides, and organic acids released by the fungi are able to participate in producing GNPs [12].

GNPs have attracted great scientific interest as a new alternative of antimicrobial agents due to the increase of antibiotic resistance traits in bacteria and other pathogens. They inhibit the growth of bacteria through collapsing cell membrane or interfering binding of tRNA to the ribosome submit, which make it very difficult for bacteria to acquire resistance against them [13].

In this study, a novel bacterial strain, identified as *Bacillus niabensis* 45, was able to synthesize GNPs from this strain's extracellular secretion. The mechanism and the optimal parameters for GNP synthesis were investigated. And the resulting GNPs were characterized by SEM-EDS, TEM-SAED, and XRD, whose antibiofilm activity was assayed.

2. Materials and Methods

2.1. Bacterial Strain and Cultivation. *Bacillus niabensis* 45 was identified by analyzing its morphologic characteristics, biochemical and physiological properties, and the 16S rDNA sequence (GenBank accession number: KT962921).

The bacterial strain was grown in starch-casein broth containing 10 g/L starch, 0.3 g/L casein, 2 g/L KNO₃, 2 g/L KH₂PO₄, 0.5 g/L MgSO₄·7H₂O, 0.02 g/L CaCO₃, and 0.001 g/L FeSO₄. Culture was incubated at 28°C for 72 h with shaking at 150 rpm.

2.2. Biosynthesis of GNPs. The fermentation broth of *B. niabensis* 45 was centrifuged at 12,000 g for 20 min. The resulting supernatant was filtered using 0.22 μm cellulose membrane. The filtrate was mixed with 2 mM of HAuCl₄ solution (9:1, v/v) and incubated at 37°C in a rotary shaker. The formation of GNPs was determined by color change and the reduction of gold ions was confirmed by UV-vis spectra observed in the range of 500–600 nm [14, 15].

2.3. Determination of Active Ingredient. The cell-free supernatant was treated with the methods of ammonium sulfate precipitation, ethyl acetate extraction, and hydrochloric acid precipitation. The ammonium sulfate precipitation was performed by adding 20%–80% saturated ammonium sulfate solution to the cell-free supernatant to yield the proteins. The resulting proteins were dissolved and dialyzed using deionized water and then applied to GNP synthesis. The acetate extraction was carried out by adding the equal volume proportion of ethyl acetate to the cell-free supernatant to obtain low polar constituents; then the organic phase was isolated and evaporated to dryness at 40°C using a rotary evaporator. The extract was dissolved in deionized water and used for GNP synthesis. The hydrochloric acid precipitation was achieved by adjusting the pH of the cell-free supernatant to 2.0 using 6 M hydrochloric acid under ice bath condition. After storing at 4°C for 12 h, the precipitate was extracted three times with acetone. The extracts were pooled and evaporated to dryness at 30°C to the crude peptides.

The crude peptides were dissolved in 50% aqueous acetonitrile/0.1 trifluoroacetic acid and applied to high-performance liquid chromatography (HPLC) equipped with a variable wavelength absorbance detector set at 214 nm (Agilent 1200, VWD) and a Shim-pack PREP-ODS C18

column (46 × 150 mm, 3.5 μm, Agilent, USA). A linear 10 to 90% acetonitrile gradient was used for elution at flow rate of 1 mL for 20 min. Eluent A consisted of 80% acetonitrile with 0.1% trifluoroacetic acid, and eluent B was composed of deionized water with 0.1% trifluoroacetic acid. All the HPLC fractions were collected separately and their activities were further assayed for GNP synthesis. The peak with the highest activity of GNP synthesis was selected for MALDI-TOF-MS and ESI-MS analysis [16]. The purified peptide was hydrolyzed by 6 M HCl for 2 h at 110°C. The hydrolyzed products were applied to thin-layer chromatography (TLC) to detect the amino groups [16].

2.4. Optimization of Parameters. The ratio of peptide (2 mg/mL) and HAuCl₄ (2 mM) which was kept in the ranges of 9:1, 8:2, 3:7, 4:6, and 5:5 (v/v) was used to find out the optimum dosage of peptide and HAuCl₄. The temperature of the reaction was investigated by incubating at 30°C, 40°C, 50°C, 60°C, 70°C, 90°C, and 100°C. The effect of pH on GNP synthesis was evaluated at pH of 4.0, 5.0, 6.0, 7.0, 8.0, 9.0, 10.0, and 11.0. The pH was maintained using 1 M HCl and 1 M NaOH. The production of GNPs was detected at various time intervals using UV-vis spectrophotometry (Agilent 8453, USA) with a resolution of 1.0 nm between 400 and 800 nm.

2.5. Characterization of GNPs. The formation of GNPs was monitored by a UV-visible spectrophotometer from 200 to 800 nm. The synthesized GNPs were separated by centrifugation and used for X-ray diffraction (XRD) analysis. XRD patterns were collected in the range of 20–80°C (2θ) operated at 40 kV and 30 mA (EXPLORER, GNR, Italy). The morphological analysis was performed by high-resolution transmission electron microscope (HR-TEM, JEOL JSM 100CX, Japan) at an accelerating voltage of 200 kV. Selected area electron diffraction (SAED) of GNPs was also analyzed using TEM. Particle size distribution was calculated for the synthesized nanoparticles by averaging 100 particles from TEM images using ImageJ software (<https://imagej.nih.gov/ij/>).

2.6. Assay of Antibiofilm Activity. The antibiofilm activity of GNPs against *P. aeruginosa* PAO1 and *S. aureus* ATCC 25923 was assayed as described in our previous study [17]. Briefly, the bacterial strains were grown at 37°C in Brain Heart Infusion (BHI) broth. The culture was diluted at 1:200 in fresh BHI broth containing various concentrations of GNPs (2048, 256, and 32 μg/well) and dispensed in sub-200 μL volumes into a 96-well microtiter plate. The plates were incubated at 37°C for 36 h. The cell growth was monitored at set intervals in 24 h using a microtiter plate reader at 600 nm. Then the residual medium in the plates was removed and the wells were washed by distilled water for three times. After drying, the attached cells were stained with 200 μL of crystal violet solution (1%, w/v) for 10 min. Subsequently, the crystal violet was removed and the plates were washed by distilled water for three times. The biofilm formation was recorded by micrograph. After photographing, the stained cells were destained using ethanol-acetone solution (4:1) to the wells. The medium without GNPs was used as a positive

control. Biofilm formation was determined by measuring the absorbance at 570 nm ($A_{570\text{nm}}$) using a microtiter plate reader. All the experiments were carried out in triplicate. The antibiofilm activity was described by the percentage of biofilm inhibition, which was calculated as follows: biofilm inhibition (%) = $[1 - (A_{\text{sample}} - A_{\text{control}})] \times 100$.

3. Results and Discussion

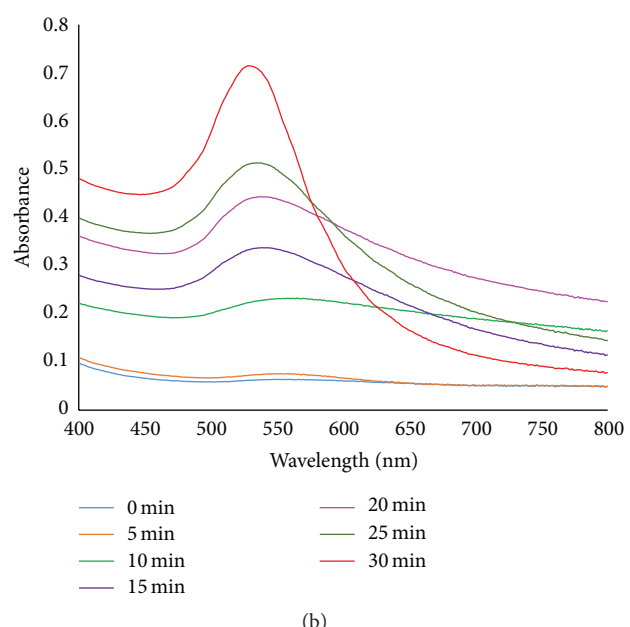
3.1. Extracellular Biosynthesis of GNPs. The bottle containing the cell-free filtrate and HAuCl₄ solution showed gradual change in color of reaction mixture from colorless to wine red with intensity increasing during the incubation period. The negative control containing starch-casein medium and HAuCl₄ solution did not show the characteristic change in color (Figure 1(a)). UV-vis spectra of the reaction mixture showed a shift of peak maxima from 528 nm to 558 nm with the increase of reaction time, and the maximum intensity was observed at 528 nm after 30 min (Figure 1(b)). Then no further change in spectra was recorded indicating completed reduction of gold ions by the filtrate. The change in the shift of peak may be possible due to variation in shape and size of GNPs [18].

3.2. Active Ingredient and Mechanism Perspective for GNP Synthesis. After treatment with the cell-free extract of *B. niabensis* 45 using different methods, only the peptide solution from hydrochloric acid precipitation exhibited an ability of GNP synthesis. This meant that peptides may be active ingredient in supernatant of *B. niabensis* 45 for biosynthesis of GNPs. Then the possible crude peptide solution was applied to PREP-HPLC. Two main peaks (P1 and P2) were separated and used to assay the activity of GNP synthesis (Figure 2(a)). It was found that only peak P2 could synthesize GNPs. The molecular weight of P2 was determined by MALDI-TOF-MS. The protonated molecular ion ($M + H$)⁺ peak of P2 was detected as 1123.22; it indicated that the molecular weight of P2 was 1122 Da (Fig. S1a in Supplementary Material available online at <http://dx.doi.org/10.1155/2016/2781347>). Then P2 was further detected by ESI-MS. The full scan spectrum gave single, double, and ternary protonated molecular ion at m/z 1123.4 ($M + H$)⁺, 561.8 ($M + 2H$)²⁺, and 375.0 ($M + 3H$)³⁺, respectively (Fig. S1b). The results are consistent with the molecular weight obtained from MALDI-TOF-MS. TLC assay of P2 showed that the colorized dots appeared at TLC plates sprayed with ninhydrin after hydrochloric acid hydrolysis, which indicate the presence of the free amino groups. But no dots were observed without acid hydrolysis. These results indicated that the compound P2 may be a cyclic peptide (Figure 2(b)).

The previous studies have revealed that amino acids and oligopeptides could act as reducing and capping agents for GNPs [19]. Based on these reports, proteins and amino acid residues in peptide such as cysteine, tyrosine, and tryptophan were found to play an important role in biosynthesis and stabilization of GNPs [20–22]. Tryptophan can produce metal NPs at basic pH by providing an electron from a transient tryptophyl radical due to conversion of tryptophan residue present in peptide [22]. In addition, it was recently reported



(a)



(b)

FIGURE 1: (a) Cell-free filtrate of *B. niabensis* 45 (left) and biosynthesized GNPs using cell-free filtrate of *B. niabensis* 45 (right). (b) UV-vis spectra of GNPs at different reaction time intervals.

that peptide containing histidine and tyrosine can mediate synthesis of silver nanoparticles (AgNPs) by electron transfer in the presence of chloride ions. In this process, histidine could bind Ag⁺ by its imidazole group to form Ag⁺-peptides. The tyrosine was used as an electron donor. The chloride ions could facilitate electron transfer-induced synthesis of AgNPs from Ag⁺-peptides by assembling Ag⁺ into AgCl microcrystals [23]. Similarly, the mechanism on rapid biosynthesis of GNPs using the peptide from *B. niabensis* 45 may be proposed as follows: the amphiprotic peptide will present the negative charge of COO⁻ group, which was in favor of the formation of Au³⁺-peptide complex. Then tyrosine or tryptophan in peptides possibly provides electrons to reduce Au³⁺ ions to Au⁰ atoms. Furthermore, GNPs may be synthesized by the aggregation of Au⁰ atoms.

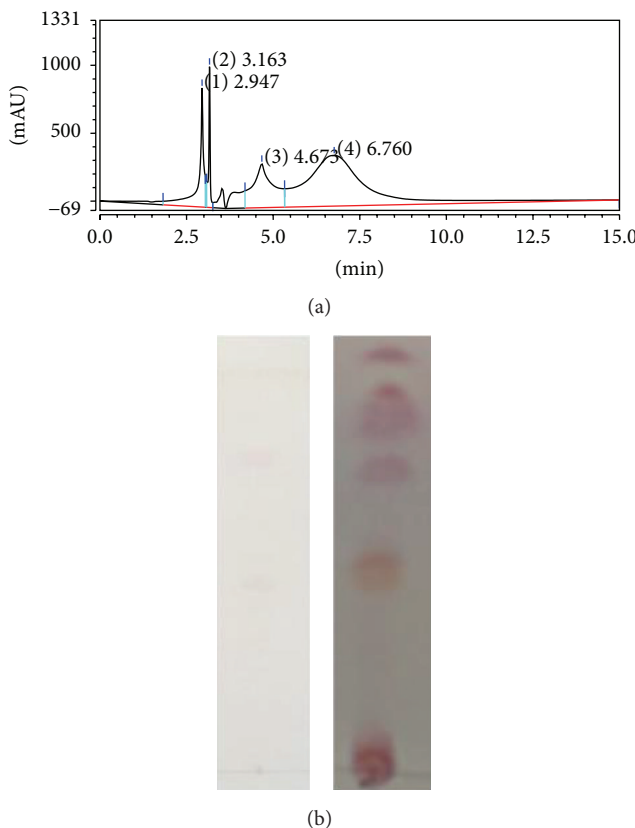


FIGURE 2: (a) PREP-HPLC profile of the crude peptides from *B. niabensis* 45. (b) TLC chromatogram of peak P2 before (left) and after (right) hydrochloric acid hydrolysis.

3.3. Optimization of Parameters for GNP Synthesis. The purified peptide P2 was used to produce GNPs and the optimum parameters of GNP synthesis were investigated. The ratio of 9 mL peptide P2 (2 mg/mL) along with 1 mL HAuCl₄ (2 mM) showed a characteristic peak at 520 nm, whereas no formation of GNPs occurred or the formation of GNPs was unstable at other concentration ratios. The effect of temperature on GNP synthesis was shown in Figure 3(a); the color of the reaction solution containing peptide P2 and HAuCl₄ turned to be wine red from colorless within 2 min when the incubated temperature was more than 40°C. UV-vis spectra of the product solution were recorded after 2 min. The maximum absorption peak shifted to 528 nm from 520 nm with the increase of the incubation temperature, and the corresponding peak intensity occurred at 100°C. These results suggested the potential of rapid biosynthesis using peptide P2 from *B. niabensis* 45 at a higher temperature. Some reports have indicated that the rate of GNP synthesis increased with an increase in reaction temperature due to increase of activation energy and reducing power of the biological moieties [24].

The ability of peptide P2 to synthesize GNPs was evaluated in the range of pH from 4.0 to 11.0 at 40°C. In this case, the rapid biosynthesis of GNPs was observed in a wide pH range of 6.0–10.0 within 5 min (Figure 3(b)). Because the peptide was amphoteric, its carboxylic groups will be protonated when the solution pH is less than isoelectric point (PI)

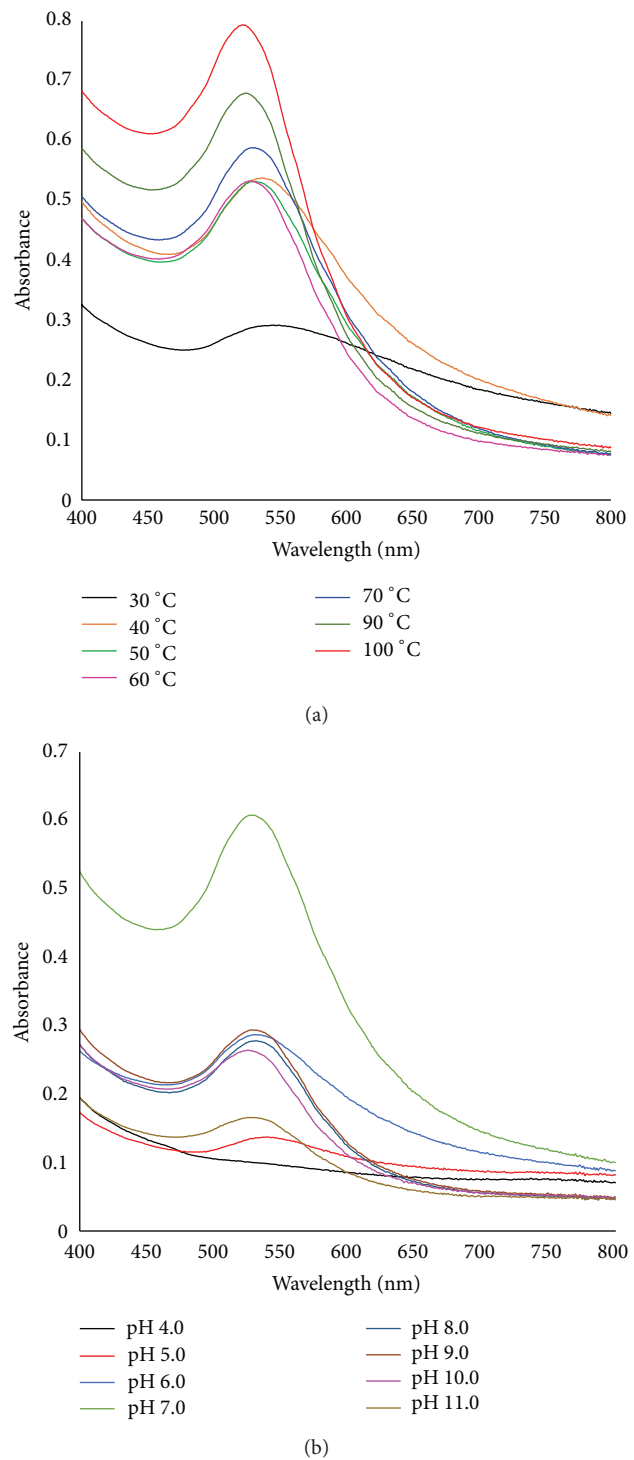


FIGURE 3: The effects of temperature (a) and pH (b) on synthesis of GNPs by peptide P2.

of the peptide, and the electrostatic repulsion cannot impart stability to particles in solution, leading to either no synthesis or instability to the particles. On the contrary, the carboxylic groups will be ionized to COO⁻ when the solution pH is more than PI of the peptide. The negative charge of carboxylic

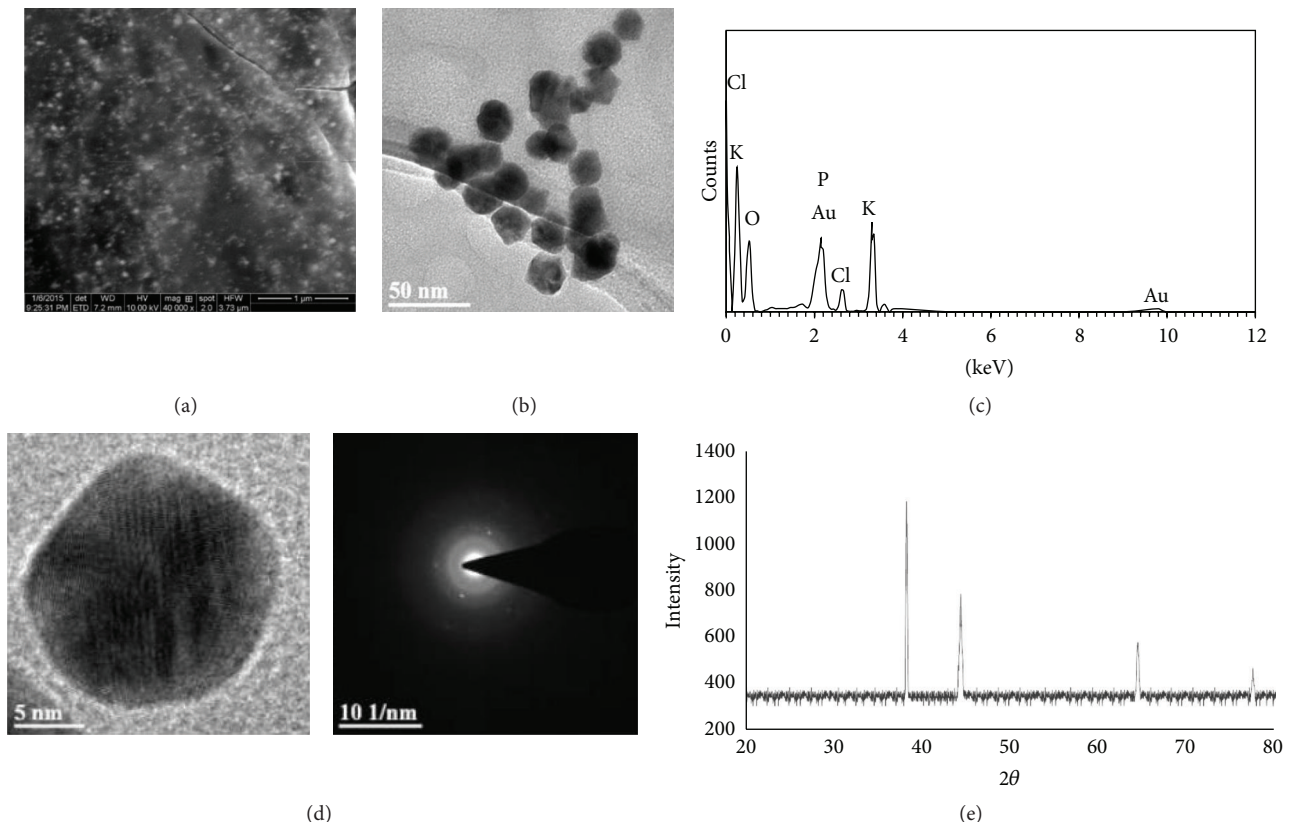


FIGURE 4: Characterization of GNPs described by SEM (a) and TEM (b) micrograph, ESD spectrum (c), SAED (d), and XRD (e) pattern.

groups would exhibit remarkable binding affinity for Au^{3+} , which may be in favor of reduction of gold ions. In addition, the maximum formation of GNPs was observed at pH 7.0 due to the presence of GNPs being stable under this condition.

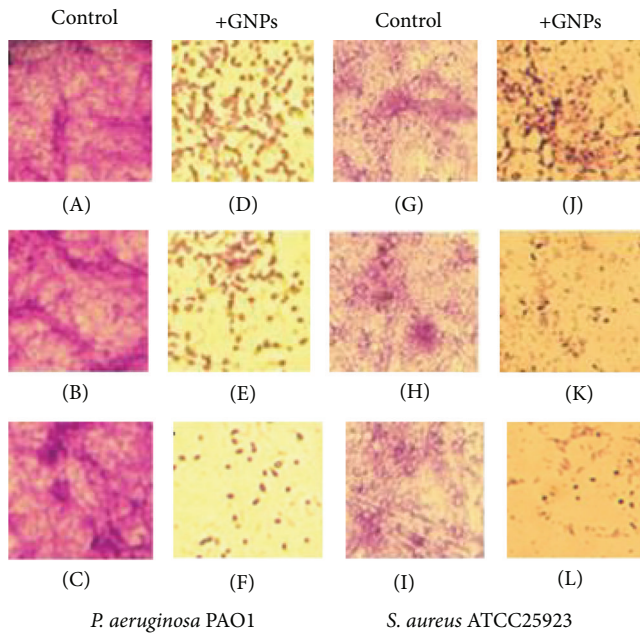
3.4. Characterization of GNPs. The SEM image showed that the morphology of GNPs was spherical (Figure 4(a)). TEM micrograph further confirmed the formation of spherical nanoparticles with the size in the range of 10–20 nm (Figure 4(b)). EDS spectrum confirmed the presence of element gold (Figure 4(c)). SAED patterns for the single particle revealed a characteristic polycrystalline ring pattern for a face-centred-cubic structure (Figure 4(d)). XRD pattern revealed broadening of the intense peaks corresponding to (111), (200), (220), and (311) Bragg reflection at $2\theta = 38.2^\circ$, 44.3° , 64.4° , and 77.5° , respectively, indicating the formation of crystalline GNPs (Figure 4(e)).

3.5. Antibiofilm Activity. As shown in Figure 5(a), GNPs could reduce the process of biofilm formation against the Gram-positive *S. aureus* ATCC25923 and the Gram-negative *P. aeruginosa* PAO1 in a dose-dependent manner without affecting cell growth (Figures 6(a) and 6(b)). The highest antibiofilm activity was exhibited against *S. aureus* and *P. aeruginosa* with inhibition percentages of up to 68% and 72%, respectively (Figure 5(b)). These data mean that GNPs

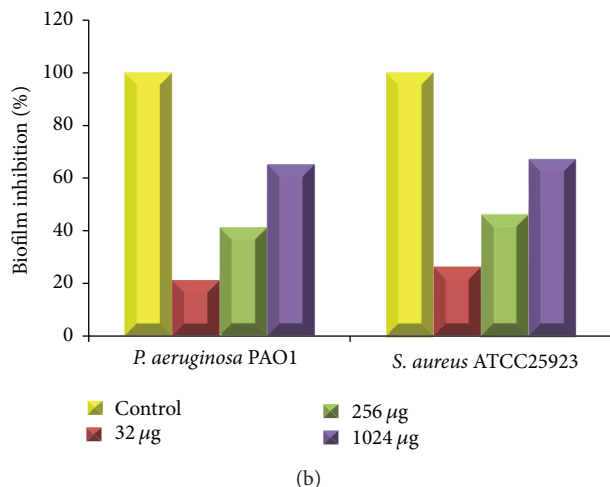
synthesized by the cyclic peptide P2 have excellent capability of antibiofilm with low toxicity or without toxicity, which may be due to the peptide coating of NPs. Our results were in agreement with the report of Salunke et al., where gold nanoparticles produced by biological extract consisting of proteins could exhibit effective inhibition against biofilm formation of *S. aureus* [25]. In fact, microbial peptides have been a new tool for antibiofilm in recent decades [26, 27]. Moreover, control of bacterial biofilms using NPs like zinc oxide and silver has attracted significant research interest because of their high surface-to-volume ratio [28–30].

4. Conclusions

In this paper, the extracellular synthesis of GNPs by *B. niabensis* 45 was investigated in detail. The active ingredient in the cell-free extract for biosynthesis of GNPs was a cyclic peptide with a molecular weight of 1122 Da, which was able to synthesize GNPs through possible electron transfer process. Then a novel protocol for rapid biosynthesis of GNPs using the cyclic peptide was demonstrated and the resulting GNPs were characterized. The biosynthesis of GNPs was obtained when 9 mL of peptide P2 (2 mg/mL) and 1 mL of HAuCl_4 solution (2 mM) were mixed together. This process was facilitated by a high temperature ($>40^\circ\text{C}$) and a wide pH range (6.0–10.0), which could significantly shorten the



(a)



(b)

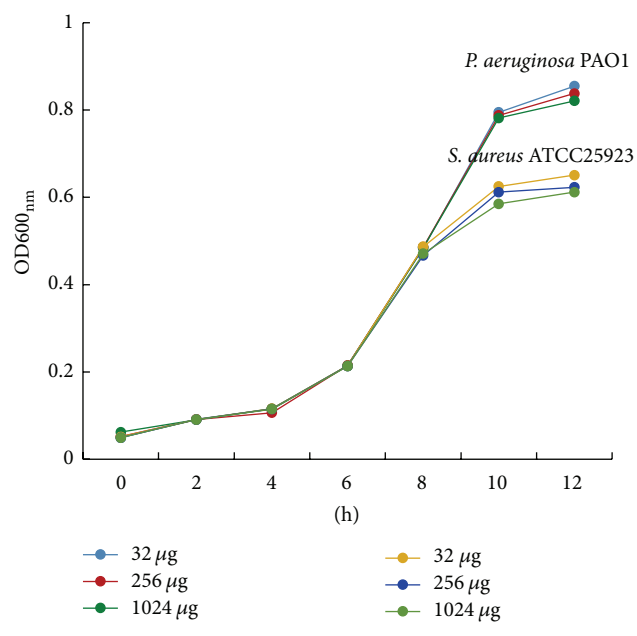
FIGURE 5: Micrographs of biofilm formation (a) and biofilm inhibition by different concentrations of GNPs (b).

reaction time to be 2–5 min. In addition, the characterization of GNPs showed that their crystals are face-centred-cubic with a size of 10–20 nm, which showed prominent antibiofilm activity against the tested Gram bacteria.

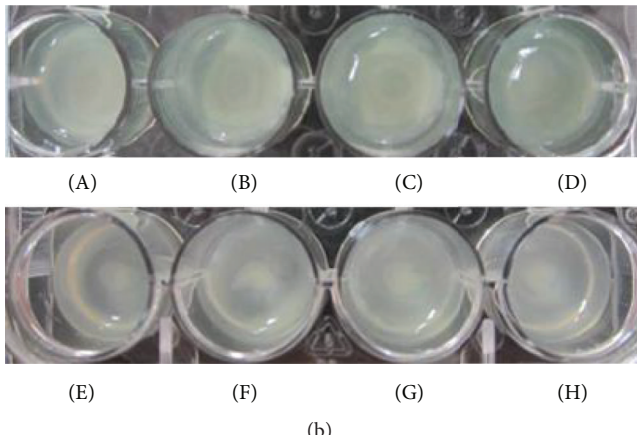
These results will lay a foundation to clarify the mechanism on microbial synthesis of GNPs and present a novel promising approach for simple and rapid biosynthesis of GNPs using microbial peptides. And the peptide coating of GNPs may be a new tool to combat bacteria biofilm.

Competing Interests

The authors declare that they have no competing interests.



(a)



(b)

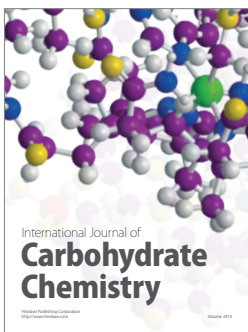
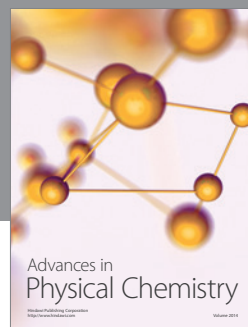
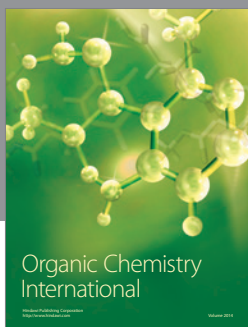
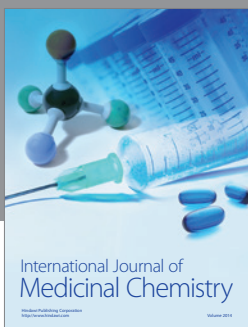
FIGURE 6: Growth profiles of the bacterial strains in 12 h (a). Comparison of cell growth in the presence of different concentrations of GNPs at 12 h (b). The upper and lower graphs represent cell growth of *P. aeruginosa* PAO1 and *S. aureus* ATCC25923, respectively. The graphs (A) and (E) are positive controls by erythromycin; (B) and (F), (C) and (G), and (D) and (H) represent the presence of 32, 256, and 2024 μg of GNPs, respectively.

Acknowledgments

The authors acknowledge the financial support provided by National Natural Science Foundation of China (Project no. 31300045), a project of Shandong Province Higher Educational Science and Technology Program (YE13), Foundation of University of Jinan (XKY1324, 1422), China Postdoctoral Science Foundation (2015M572018), and Open fund of Xinjiang Production & Construction Corps Key Laboratory of Protection and Utilization of Biological Resources in Tarim Basin (BYBR1405).

References

- [1] S. K. Ghosh and T. Pal, "Interparticle coupling effect on the surface plasmon resonance of gold nanoparticles: from theory to applications," *Chemical Reviews*, vol. 107, no. 11, pp. 4797–4862, 2007.
- [2] G. Ajnai, A. Chiu, T. Kan, C.-C. Cheng, T.-H. Tsai, and J. Chang, "Trends of gold nanoparticle-based drug delivery system in cancer therapy," *Journal of Experimental and Clinical Medicine*, vol. 6, no. 6, pp. 172–178, 2014.
- [3] X. Qian, X.-H. Peng, D. O. Ansari et al., "In vivo tumor targeting and spectroscopic detection with surface-enhanced Raman nanoparticle tags," *Nature Biotechnology*, vol. 26, no. 1, pp. 83–90, 2008.
- [4] A. Gerber, M. Bundschuh, D. Klingelhofer, and D. A. Groneberg, "Gold nanoparticles: recent aspects for human toxicology," *Journal of Occupational Medicine and Toxicology*, vol. 8, no. 1, article 32, 2013.
- [5] N. I. Hulkoti and T. C. Taranath, "Biosynthesis of nanoparticles using microbes—a review," *Colloids and Surfaces B: Biointerfaces*, vol. 121, pp. 474–483, 2014.
- [6] A. Mishra, M. Kumari, S. Pandey, V. Chaudhry, K. C. Gupta, and C. S. Nautiyal, "Biocatalytic and antimicrobial activities of gold nanoparticles synthesized by *Trichoderma sp.*," *Bioresource Technology*, vol. 166, pp. 235–242, 2014.
- [7] T. J. Beveridge and R. G. E. Murray, "Sites of metal deposition in the cell wall of *Bacillus subtilis*," *Journal of Bacteriology*, vol. 141, no. 2, pp. 876–887, 1980.
- [8] P. Mukherjee, S. Senapati, D. Mandal et al., "Extracellular synthesis of gold nanoparticles by the fungus *Fusarium oxysporum*," *ChemBioChem*, vol. 3, no. 5, pp. 461–463, 2002.
- [9] S. He, Z. Guo, Y. Zhang, S. Zhang, J. Wang, and N. Gu, "Biosynthesis of gold nanoparticles using the bacteria *Rhodopseudomonas capsulata*," *Materials Letters*, vol. 61, no. 18, pp. 3984–3987, 2007.
- [10] M. Sastry, A. Ahmed, M. Khan, and R. Kumar, "Biosynthesis of metal nanoparticles using fungi and actinomycete," *Current Science*, vol. 85, no. 2, pp. 162–170, 2003.
- [11] R. Sanghi, P. Verma, and S. Puri, "Enzymatic formation of gold nanoparticles using *Phanerochaete chrysosporium*," *Advances in Chemical Engineering and Science*, vol. 1, pp. 154–162, 2011.
- [12] D. S. Balaji, S. Basavaraja, R. Deshpande, D. B. Mahesh, B. K. Prabhakar, and A. C. Venkataraman, "Extracellular biosynthesis of functionalized silver nanoparticles by strains of *Cladosporium cladosporioides* fungus," *Colloids and Surfaces B: Biointerfaces*, vol. 68, no. 1, pp. 88–92, 2009.
- [13] Y. Cui, Y. Zhao, Y. Tian, W. Zhang, X. Lü, and X. Jiang, "The molecular mechanism of action of bactericidal gold nanoparticles on *Escherichia coli*," *Biomaterials*, vol. 33, no. 7, pp. 2327–2333, 2012.
- [14] J. Y. Song, H.-K. Jang, and B. S. Kim, "Biological synthesis of gold nanoparticles using *Magnolia kobus* and *Diopyros kaki* leaf extracts," *Process Biochemistry*, vol. 44, no. 10, pp. 1133–1138, 2009.
- [15] L. Du, L. Xian, and J. X. Feng, "Rapid extra-/intracellular biosynthesis of gold nanoparticles by the fungus *Penicillium sp.*," *Journal of Nanoparticle Research*, vol. 13, no. 3, pp. 921–930, 2011.
- [16] Y. H. Han, B. Zhang, Q. Shen et al., "Purification and identification of two antifungal cyclic peptides produced by *Bacillus amyloliquefaciens* L-H15," *Applied Biochemistry and Biotechnology*, vol. 176, no. 8, pp. 2202–2212, 2015.
- [17] Y. M. Li, Q. Li, D. K. Hao et al., "Production, purification, and antibiofilm activity of a novel exopolysaccharide from *Arthrobacter sp. B4*," *Preparative Biochemistry & Biotechnology*, vol. 45, no. 3, pp. 192–204, 2015.
- [18] M. V. Sujitha and S. Kannan, "Green synthesis of gold nanoparticles using Citrus fruits (*Citrus limon*, *Citrus reticulata* and *Citrus sinensis*) aqueous extract and its characterization," *Spectrochimica Acta Part A: Molecular and Biomolecular Spectroscopy*, vol. 102, pp. 15–23, 2013.
- [19] S. R. Tegture, A. U. Borse, B. R. Sankapal, V. J. Garole, and D. J. Garole, "Green biochemistry approach for synthesis of silver and gold nanoparticles using *Ficus racemosa* latex and their pH-dependent binding study with different amino acids using UV/Vis absorption spectroscopy," *Amino Acids*, vol. 47, no. 4, pp. 757–765, 2015.
- [20] D. P. Nelson, D. M. Priscyla, D. Marcela, Y. Alka, G. Aniket, and R. Mahendra, "Mechanistic aspects in the biogenic synthesis of extracellular metal nanoparticles by peptides, bacteria, fungi, and plants," *Applied Microbiology and Biotechnology*, vol. 90, no. 5, pp. 1609–1624, 2011.
- [21] D. Raju, R. Mendapara, and U. J. Mehta, "Protein mediated synthesis of Au–Ag bimetallic nanoparticles," *Materials Letters*, vol. 124, pp. 271–274, 2014.
- [22] S. Si and T. K. Manda, "Tryptophan-based peptides to synthesize gold and silver nanoparticles: a mechanistic and kinetic study," *Chemistry—A European Journal*, vol. 13, no. 11, pp. 3160–3168, 2007.
- [23] S. Kracht, M. Messerer, M. Lang et al., "Electron transfer in peptides: on the formation of silver nanoparticles," *Angewandte Chemie—International Edition*, vol. 54, no. 10, pp. 2912–2916, 2015.
- [24] C. Burda, X. Chen, R. Narayanan, and M. A. El-Sayed, "Chemistry and properties of nanocrystals of different shapes," *Chemical Reviews*, vol. 105, no. 4, pp. 1025–1102, 2005.
- [25] G. R. Salunke, S. Ghosh, R. J. Santosh Kumar et al., "Rapid efficient synthesis and characterization of silver, gold, and bimetallic nanoparticles from the medicinal plant *Plumbago zeylanica* and their application in biofilm control," *International Journal of Nanomedicine*, vol. 9, no. 1, pp. 2635–2653, 2014.
- [26] P. Jorge, A. Lourenço, and M. O. Pereira, "New trends in peptide-based anti-biofilm strategies: a review of recent achievements and bioinformatic approaches," *Biofouling*, vol. 28, no. 10, pp. 1033–1061, 2012.
- [27] M. Moryl, M. Spętana, K. Dziubek et al., "Antimicrobial, anti-adhesive and antibiofilm potential of lipopeptides synthesised by *Bacillus subtilis*, on uropathogenic bacteria," *Acta Biochimica Polonica*, vol. 62, no. 4, pp. 725–732, 2015.
- [28] A. Shrestha, S. Zhilong, N. K. Gee, and A. Kishen, "Nanoparticulates for antibiofilm treatment and effect of aging on its antibacterial activity," *Journal of Endodontics*, vol. 36, no. 6, pp. 1030–1035, 2010.
- [29] S. Gaidhani, R. Singh, D. Singh et al., "Biofilm disruption activity of silver nanoparticles synthesized by *Acinetobacter calcoaceticus* PUCM 1005," *Materials Letters*, vol. 108, pp. 324–327, 2013.
- [30] S. Ghosh, S. Jagtap, P. More et al., "*Dioscorea bulbifera* mediated synthesis of novel $\text{Au}_{\text{core}}\text{Ag}_{\text{shell}}$ nanoparticles with potent antibiofilm and antileishmanial activity," *Journal of Nanomaterials*, vol. 2015, Article ID 562938, 12 pages, 2015.



Hindawi

Submit your manuscripts at
<http://www.hindawi.com>

